The supplemental information

Derivation of the matrices M and MT

Each column vector in the matrix **M** corresponds to a crystal axis of wadsleyite with coordinates expressed with respect to the crystal axes of ringwoodite (see also Figure 8). When expressed in terms of the cubic crystal axis system of ringwoodite, the crystal axes of wadsleyite correspond to the following vectors:

$$\mathbf{a}_{\mathrm{wds}} = \frac{1}{2}\cdot\mathbf{a}_{\mathbf{1}\mathrm{rwd}} - \frac{1}{2}\cdot\mathbf{a}_{\mathbf{2}\mathrm{rwd}} + 0\cdot\mathbf{a}_{\mathbf{3}\mathrm{rwd}} = \frac{1}{2}\begin{pmatrix}1\\-1\\0\end{pmatrix}$$

$$\mathbf{b}_{\mathrm{wds}} = 1\cdot\mathbf{a}_{\mathbf{1}\mathrm{rwd}} + 1\cdot\mathbf{a}_{\mathbf{2}\mathrm{rwd}} + 0\cdot\mathbf{a}_{\mathbf{3}\mathrm{rwd}} = \frac{1}{2}\begin{pmatrix}2\\2\\0\end{pmatrix}$$

$$\mathbf{c}_{\mathrm{wds}} = 0\cdot\mathbf{a}_{\mathbf{1}\mathrm{rwd}} + 0\cdot\mathbf{a}_{\mathbf{2}\mathrm{rwd}} + 1\cdot\mathbf{a}_{\mathbf{3}\mathrm{rwd}} = \frac{1}{2}\begin{pmatrix}0\\0\\2\end{pmatrix}$$

The lengths of these vectors are:

$$a_{\mathrm{wds}} = |\mathbf{a}_{\mathrm{wds}}| = |\mathbf{a}_{\mathrm{rwd}}|\sqrt{\left(\frac{1}{2}\right)^2 + \left(-\frac{1}{2}\right)^2} = \frac{|\mathbf{a}_{\mathrm{rwd}}|}{\sqrt{2}} = \frac{a_{\mathrm{rwd}}}{\sqrt{2}}$$

$$b_{\mathrm{wds}} = |\mathbf{b}_{\mathrm{wds}}| = |\mathbf{a}_{\mathrm{rwd}}|\sqrt{1^2+1^2} = |\mathbf{a}_{\mathrm{rwd}}|\sqrt{2} = 2\frac{|\mathbf{a}_{\mathrm{rwd}}|}{\sqrt{2}} = 2\frac{a_{\mathrm{rwd}}}{\sqrt{2}} = 2a_{\mathrm{wds}}$$

$$c_{\mathrm{wds}} = |\mathbf{c}_{\mathrm{wds}}| = |\mathbf{a}_{\mathrm{rwd}}|\sqrt{1^2} = |\mathbf{a}_{\mathrm{rwd}}| = a_{\mathrm{rwd}} = a_{\mathrm{wds}}\sqrt{2}$$

Writing the vectors for $\mathbf{a}_{\mathrm{wds}}$, $\mathbf{b}_{\mathrm{wds}}$, and $\mathbf{c}_{\mathrm{wds}}$ as the first, second, and third column, respectively, of a 3 × 3 matrix gives the matrix **M** for transforming a vector **w** with coordinates w_1, w_2, w_3 defined with respect to the crystal axes of wadsleyite to a vector **r** in the cubic axis system of ringwoodite:

$$\mathbf{Mw} = \frac{1}{2}\begin{bmatrix}1 & 2 & 0\\-1 & 2 & 0\\0 & 0 & 2\end{bmatrix}\begin{pmatrix}w_1\\w_2\\w_3\end{pmatrix} = \begin{pmatrix}r_1\\r_2\\r_3\end{pmatrix} = \mathbf{r}$$

or alternatively written as

$$\mathbf{M}(w_1, w_2, w_3)^{\mathrm{T}}_{\mathrm{wds}} = (r_1, r_2, r_3)^{\mathrm{T}}_{\mathrm{rwd}}$$

The twin lattice (TL) is described by the parameters a_{TL} = 14.076 Å, b_{TL} = 23.137 Å, c_{TL} = 14.169 Å, α_{TL} = 89.26°, β_{TL} = 110.06°, γ_{TL} = 91.25°. The orientation of the axes spanning the twin lattice expressed relative to the crystal axes of wadsleyite is given by the matrix:

$$\mathbf{T} = \begin{bmatrix} 2 & 2 & 0 \\ 0 & 1 & -1 \\ -1 & 2 & 1 \end{bmatrix}$$

The second column of the matrix **T** is the direction of the twin axis in direct space expressed in coordinates of the crystal axis system of wadsleyite, the first and third columns are the shortest independent vectors parallel to the (122) twin plane, respectively. The matrix that transforms the coordinates of a vector in the twin lattice into the crystal axis system of ringwoodite is then obtained by matrix multiplication of the matrices **M** and **T**:

$$\mathbf{MT} = \begin{bmatrix} 1 & 2 & -1 \\ -1 & 0 & -1 \\ -1 & 2 & 1 \end{bmatrix}$$

For the matrix multiplication, we can treat each column of the matrix **T** as a vector that is being transformed by the matrix **M**. As a result, the vector $(2,0,-1)^{\mathrm{T}}_{\mathrm{wds}}$ (first column of **T**) with coordinates expressed in the crystal axis system of wadsleyite is transformed to the vector $(1,-1,-1)^{\mathrm{T}}_{\mathrm{rwd}}$ (first column of the matrix product **MT**) with coordinates expressed in the crystal axis system of ringwoodite. Similar relations exist between the second and third columns of the matrix **M** and the matrix product **MT**, i.e., $(2,1,2)^{\mathrm{T}}_{\mathrm{wds}} \rightarrow (2,0,2)^{\mathrm{T}}_{\mathrm{rwd}}$ and $(0,-1,1)^{\mathrm{T}}_{\mathrm{wds}} \rightarrow$

$(-1,-1,1)^{\mathrm{T}}_{\mathrm{rwd}}$, respectively. A vector **t** with coordinates t_1, t_2, t_3 with respect to the axes of the twin lattice, then transforms as follows:

$$\mathbf{MTt} = \begin{bmatrix} 1 & 2 & -1 \\ -1 & 0 & -1 \\ -1 & 2 & 1 \end{bmatrix} \begin{pmatrix} t_1 \\ t_2 \\ t_3 \end{pmatrix} = \begin{pmatrix} r_1 \\ r_2 \\ r_3 \end{pmatrix} = \mathbf{r}$$

Here, the vector **r** expresses the vector **t** in terms of the crystal axes of ringwoodite.

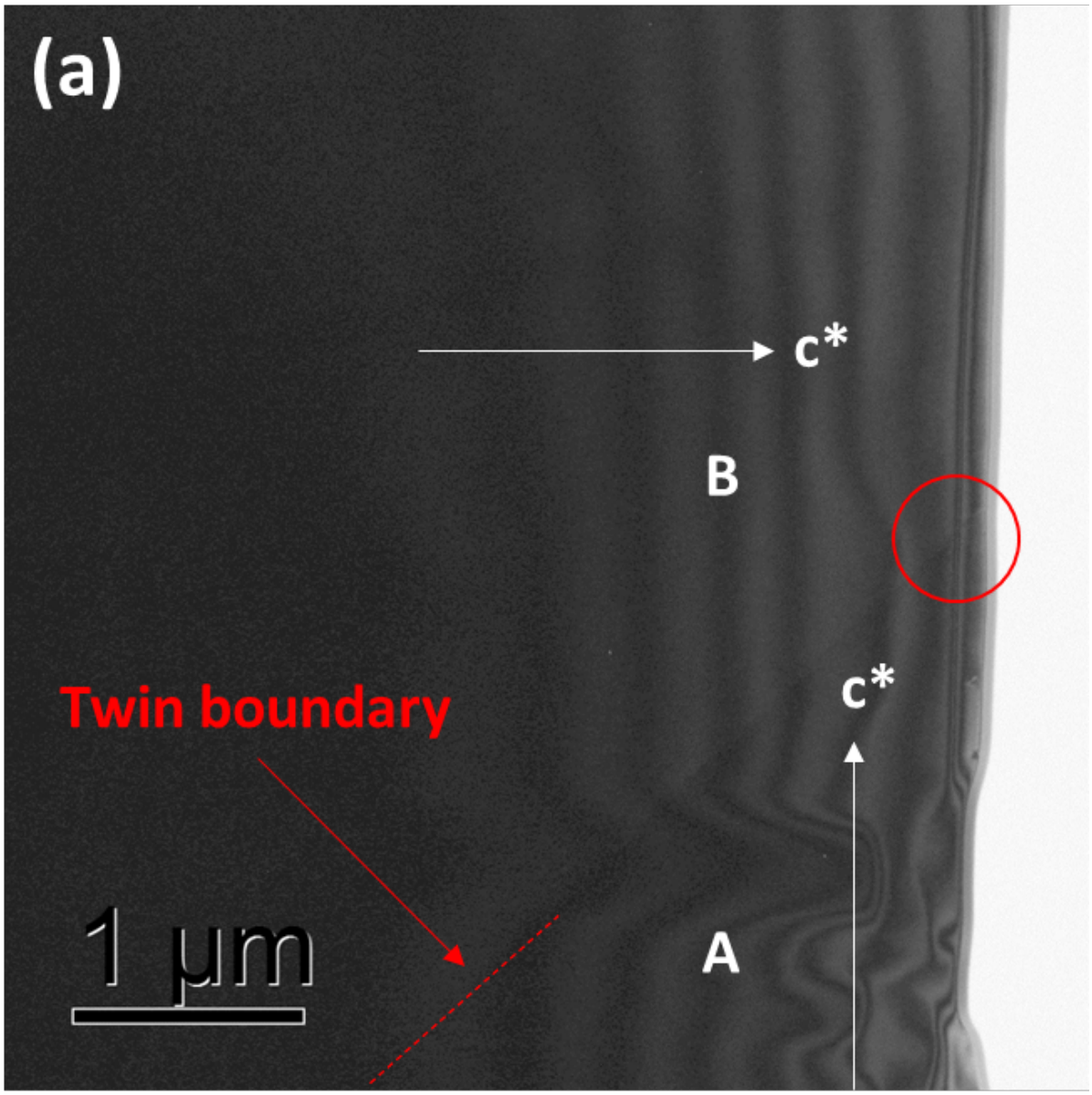

Fig. S1a

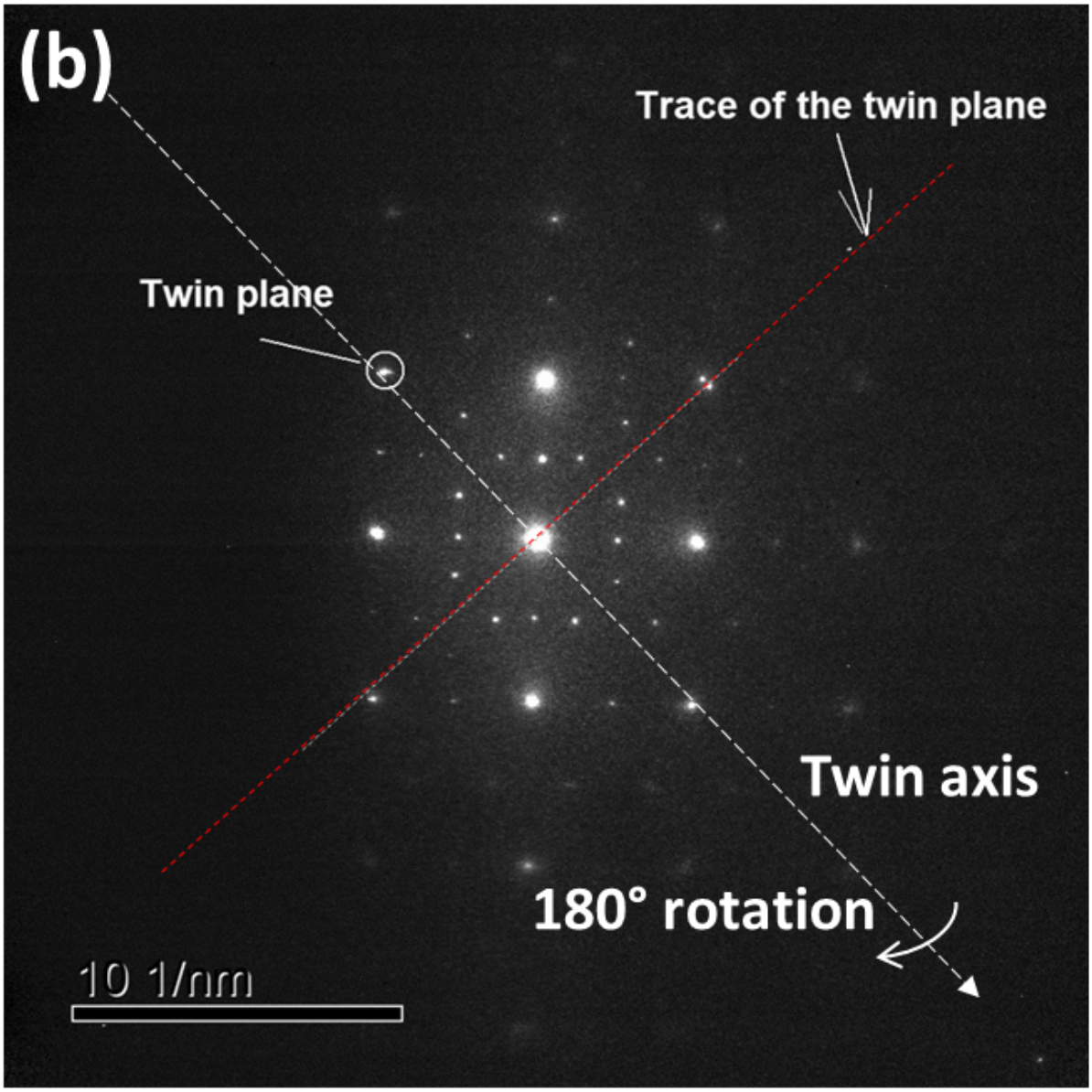
(b)
Trace of the twin plane
Twin plane
Twin axis
180° rotation
10 1/nm

Fig. S1b

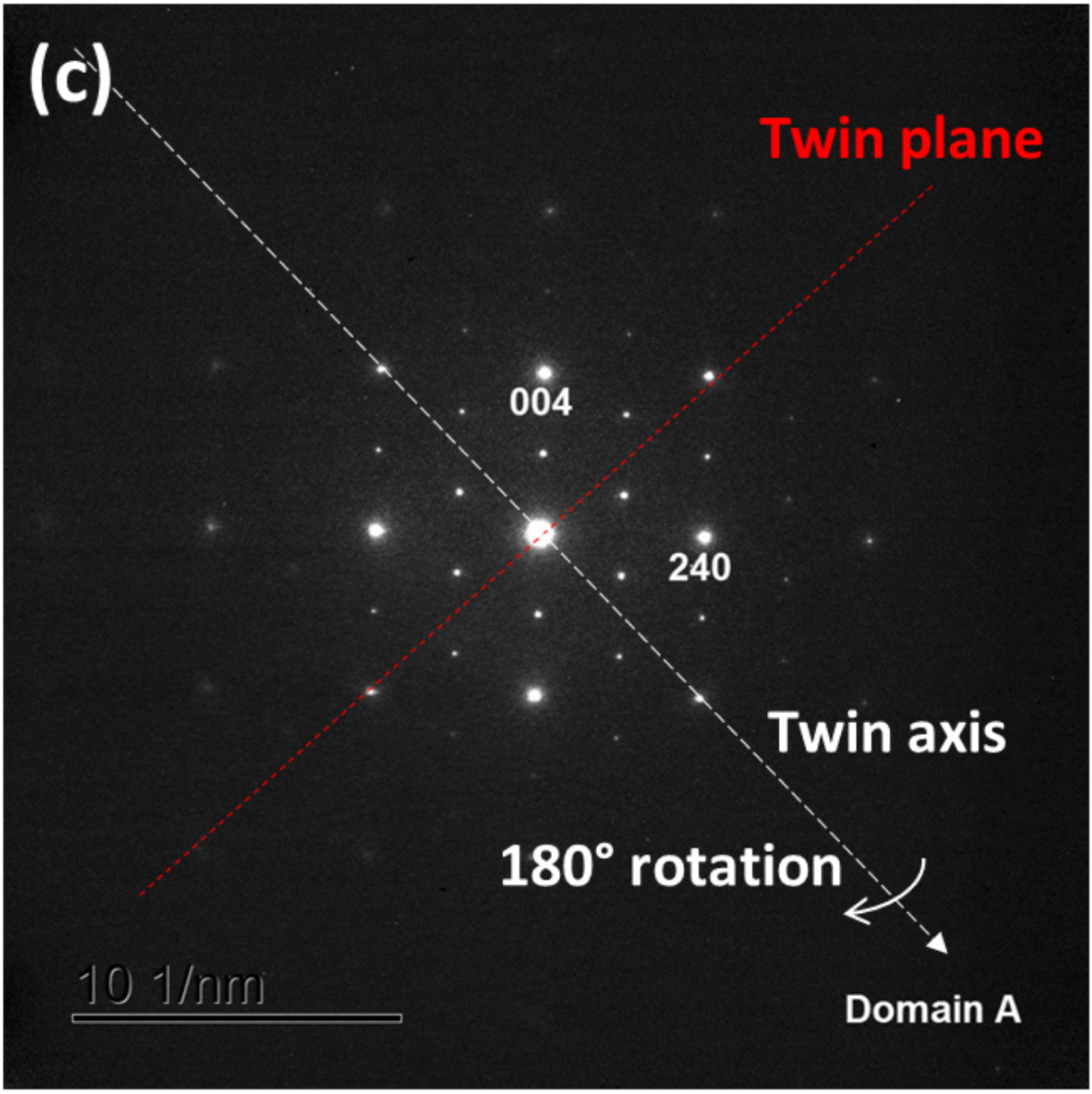

Fig. S1c

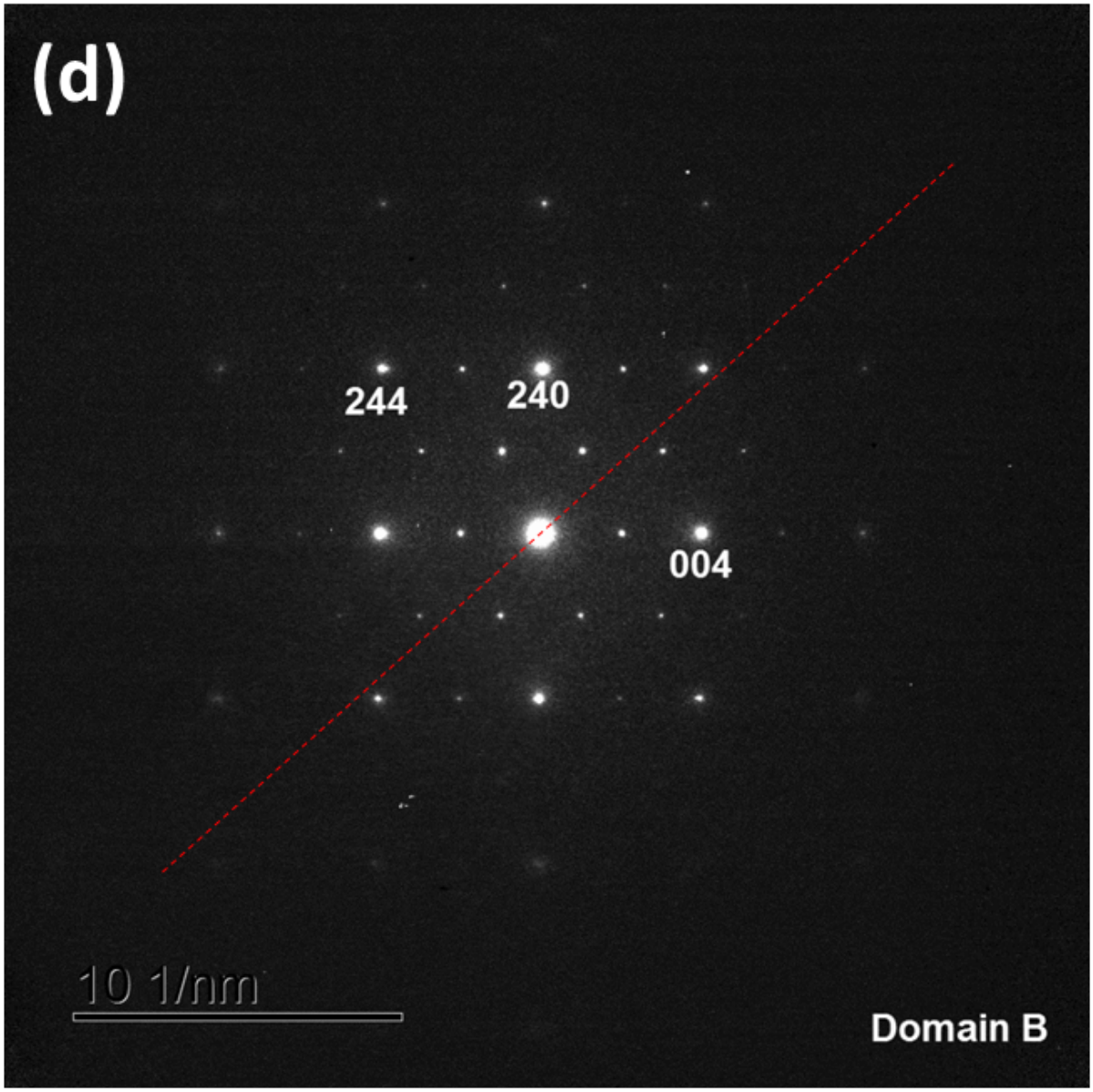

Fig. S1d

Supplemental Fig. S1. (a) Conventional bright-field TEM image of the twin, taken from the [2$\bar{1}$0] zone axis of wadsleyite. (b) Selected area electron diffraction (SAED) pattern from an area including the composition plane indicated by the red circle in (a). The corresponding SAED patterns from (c) the domain A and (d) the domain B, indicating a 180° rotation about the twin axis or a reflection on the twin plane.

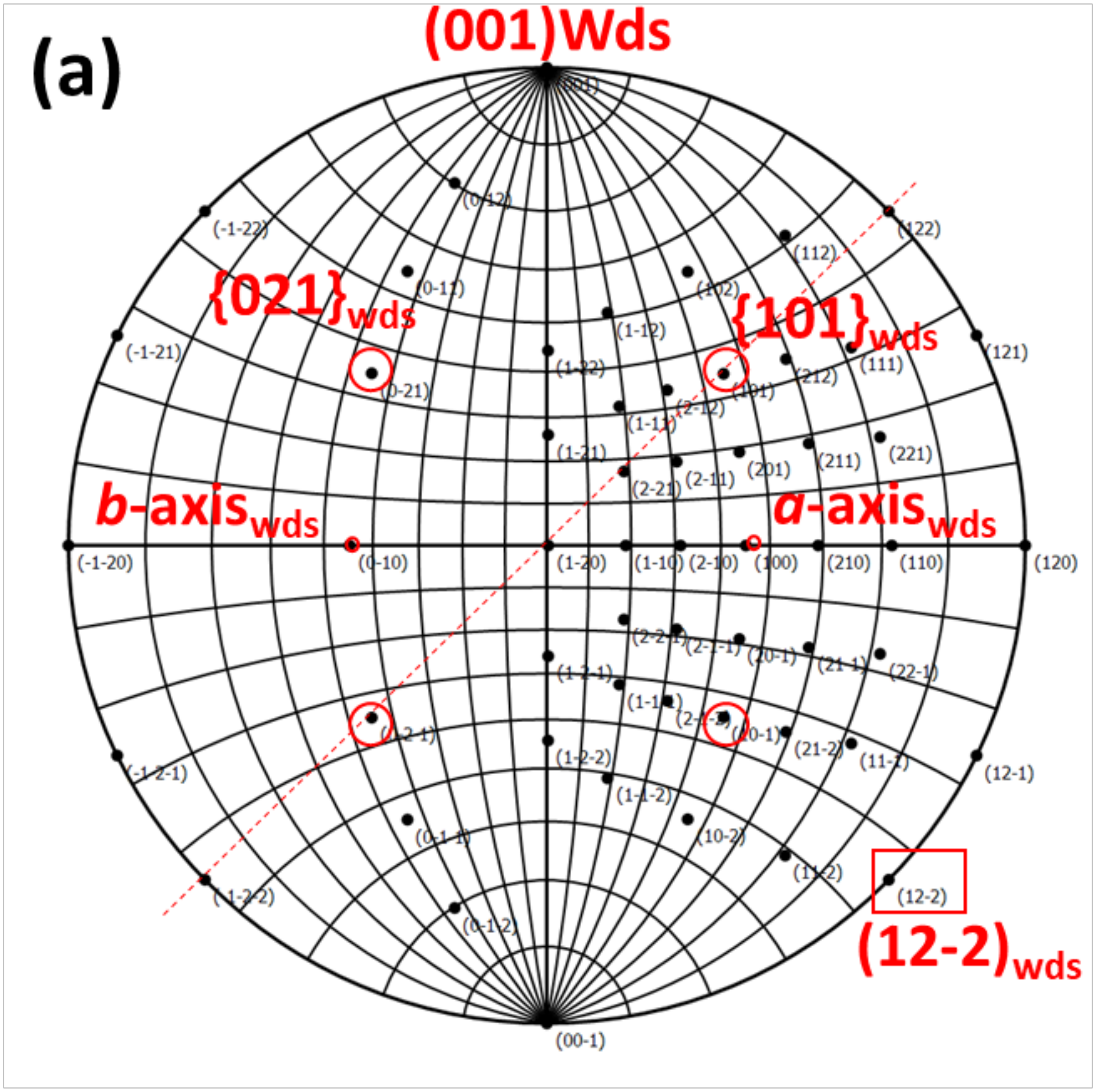
(a)
(001)Wds
{021}wds
{101}wds
b-axiswds
a-axiswds
(12-2)wds
(-1-22)
(0-12)
(122)
(112)
(0-11)
(102)
(1-12)
(-1-21)
(121)
(111)
(1-22)
(212)
(0-21)
(101)
(2-12)
(1-11)
(221)
(1-21)
(211)
(201)
(2-11)
(2-21)
(-1-20)
(0-10)
(1-20)
(1-10)
(2-10)
(100)
(210)
(110)
(120)
(2-2-1)
(2-1-1)
(20-1)
(21-1)
(22-1)
(1-2-1)
(1-1-1)
(10-1)
(21-2)
(11-1)
(12-1)
(-1-2-1)
(1-2-2)
(1-1-2)
(0-1-1)
(10-2)
(11-2)
(12-2)
(-1-2-2)
(0-1-2)
(00-1)

Fig. S2a

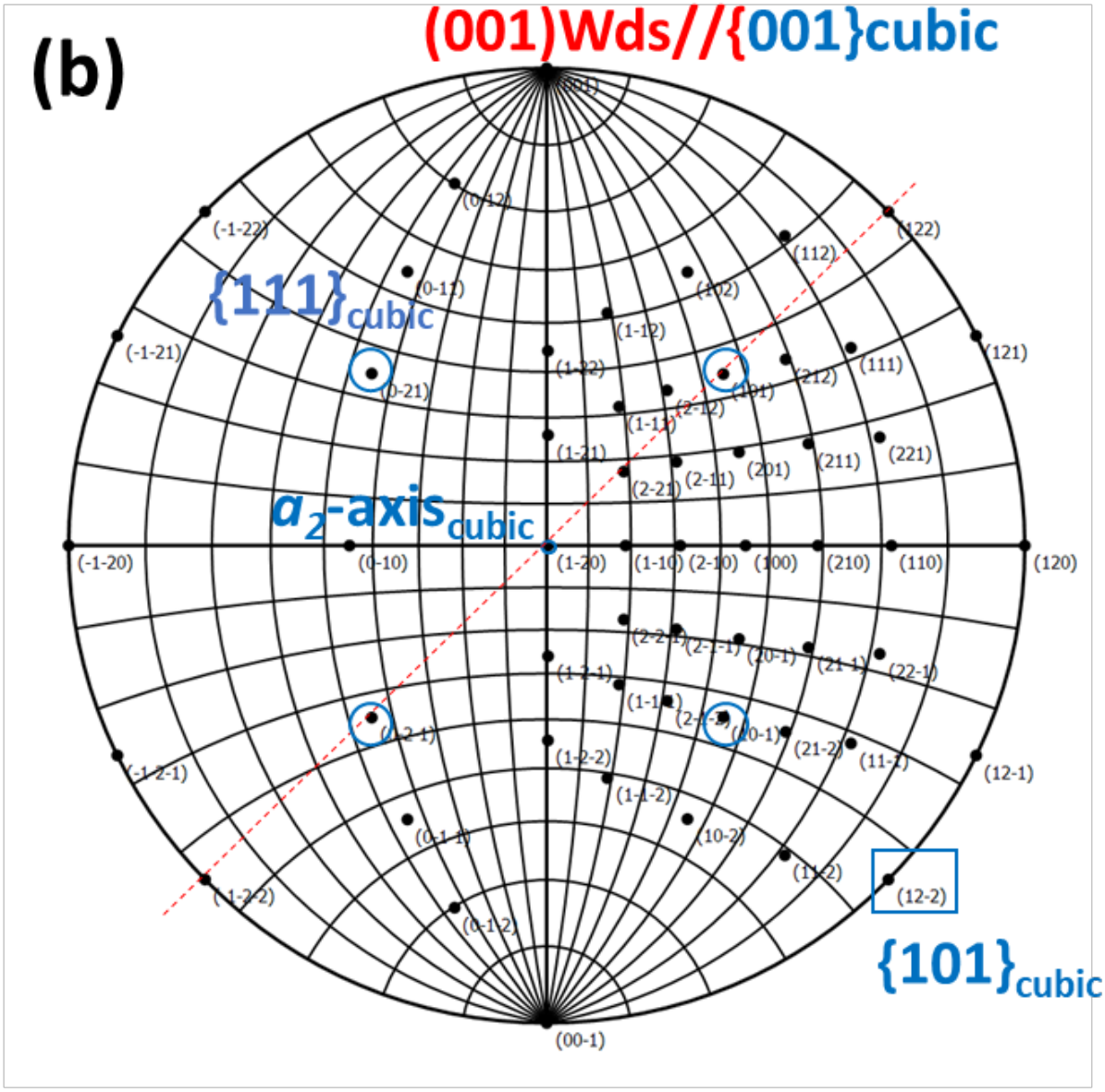

Fig. S2b

Supplemental Fig. S2. Stereographic projections along the [$2\bar{1}0$] zone axis of wadsleyite indicating the orientation of layers with close-packed oxygen anions. Poles are labelled according to the orthorhombic (a) and cubic (b) axes. Projections were indexed using the EDA software (Kogure, 2015) and the ReciPro software (Seto and Ohtsuka, 2022).

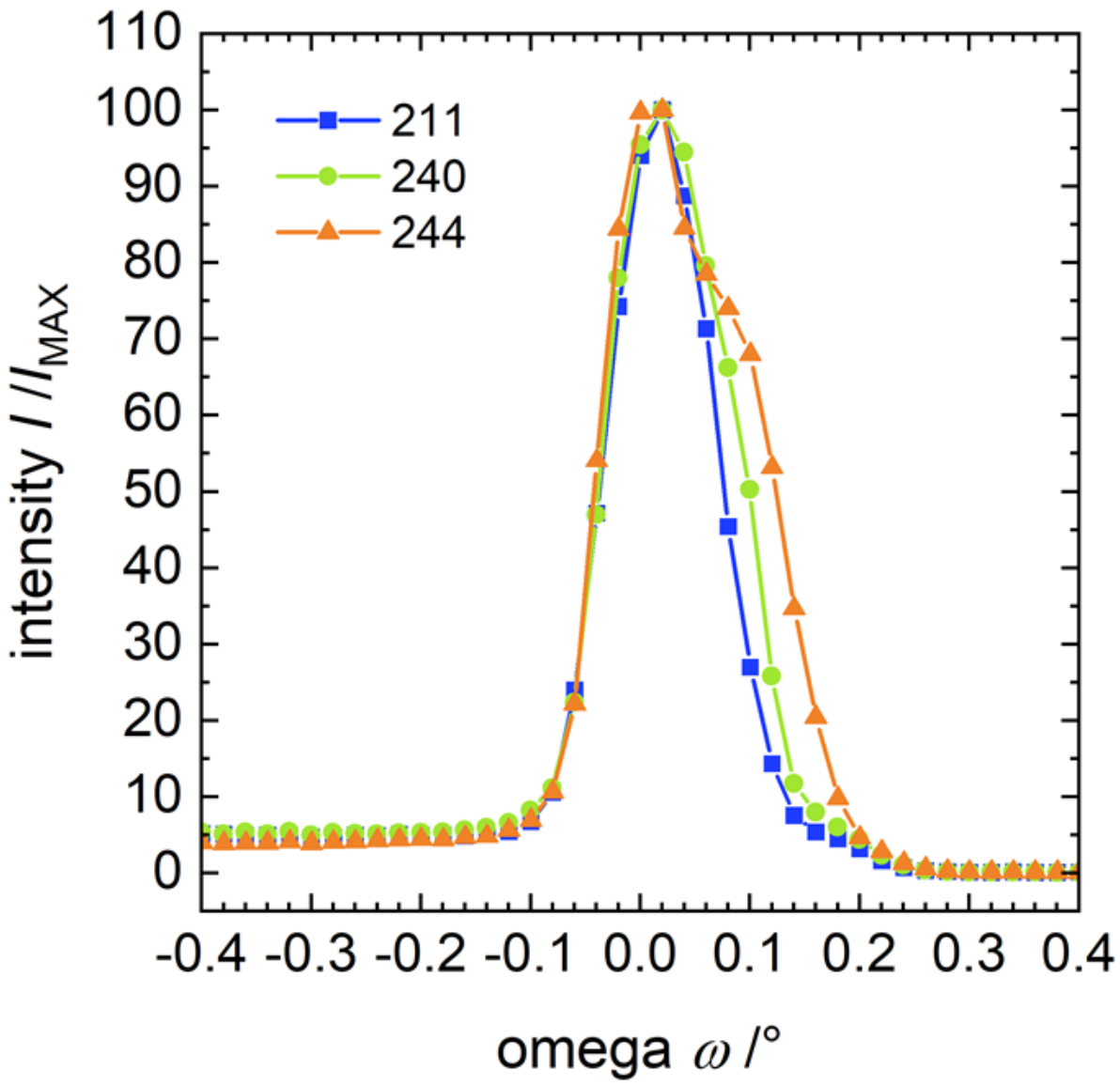

Fig. S3

Supplemental Fig. S3. Omega scans of reflections 211, 240, and 244 of a twinned wadsleyite crystal. Splitting of the 244 reflection is consistent with composition planes parallel to (122) planes.

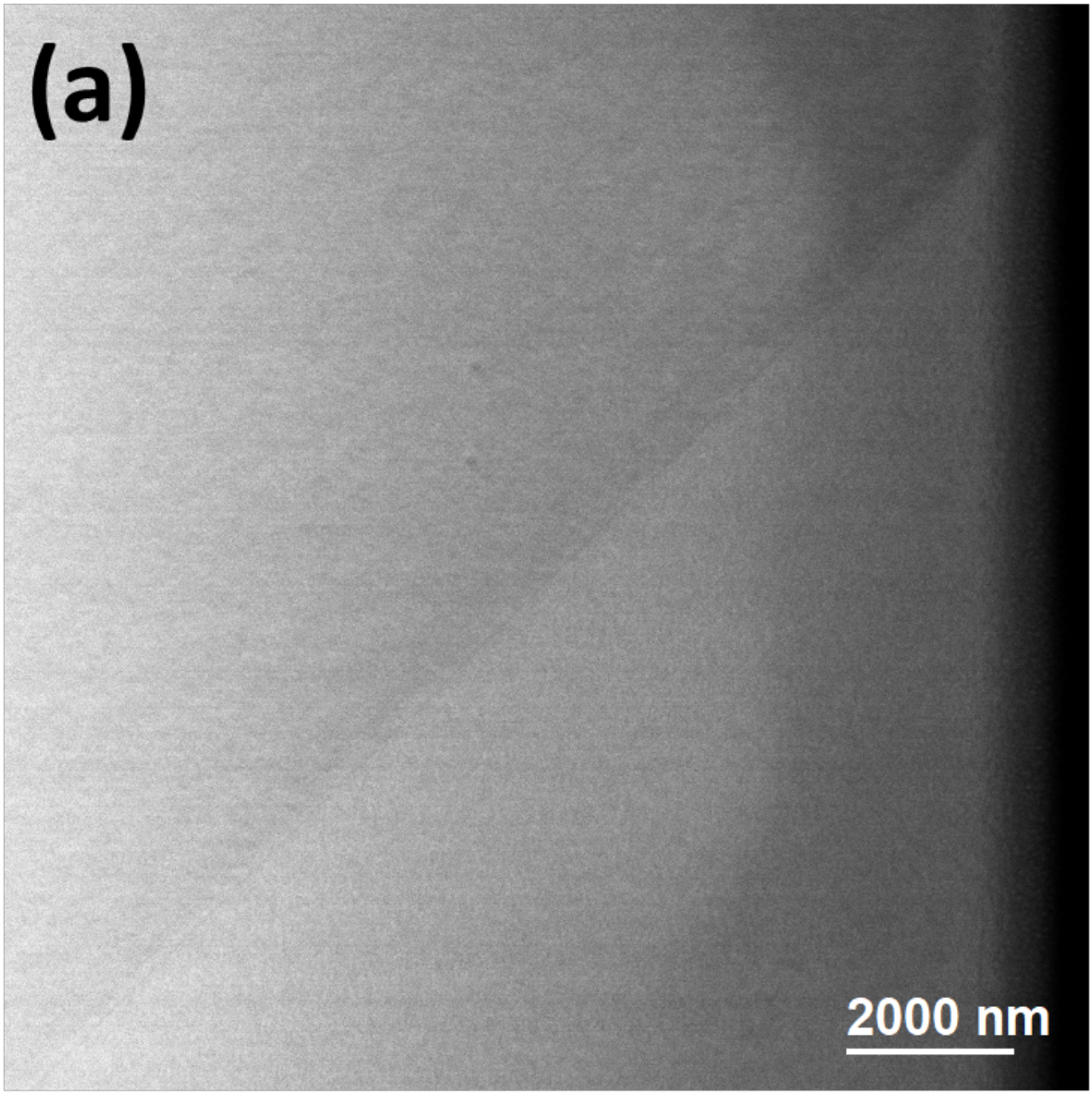

Fig. S4a

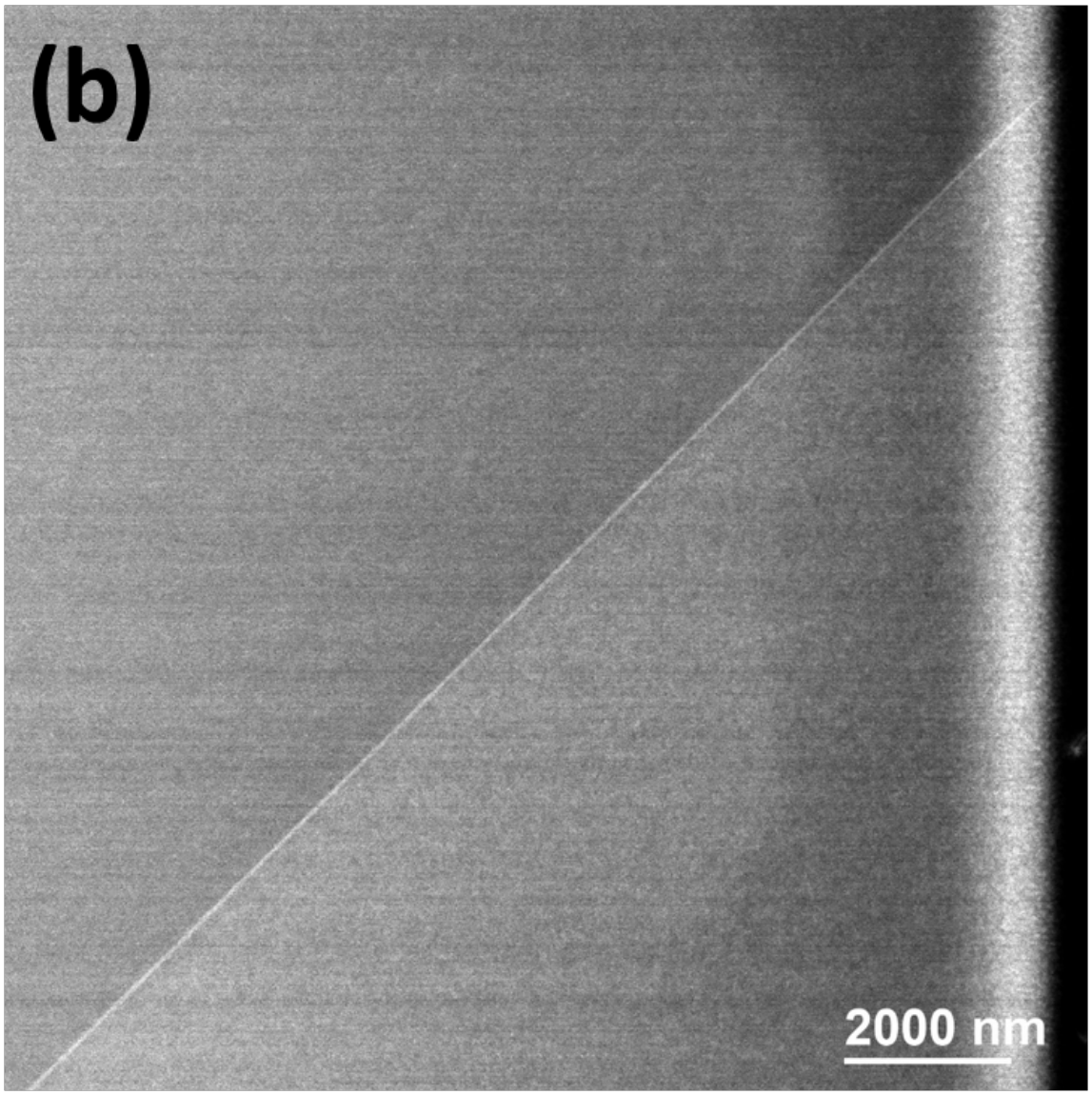

Fig. S4b

Supplemental Fig. S4. (a) HAADF-STEM and (b) dark-field STEM images of a twin in wadsleyite, taken along the [$2\bar{1}0$] zone axis. The camera length was set to 86 mm to obtain mass-thickness contrast in the HAADF image (the collection angle is from 50 to 300 mrad). (b) Diffraction contrast in the dark-field image. No chemical impurities along the composition plane are visible in the HAADF image (a) while electron irradiation damage along the composition plane becomes visible as bright contrast in the dark-field image (b).

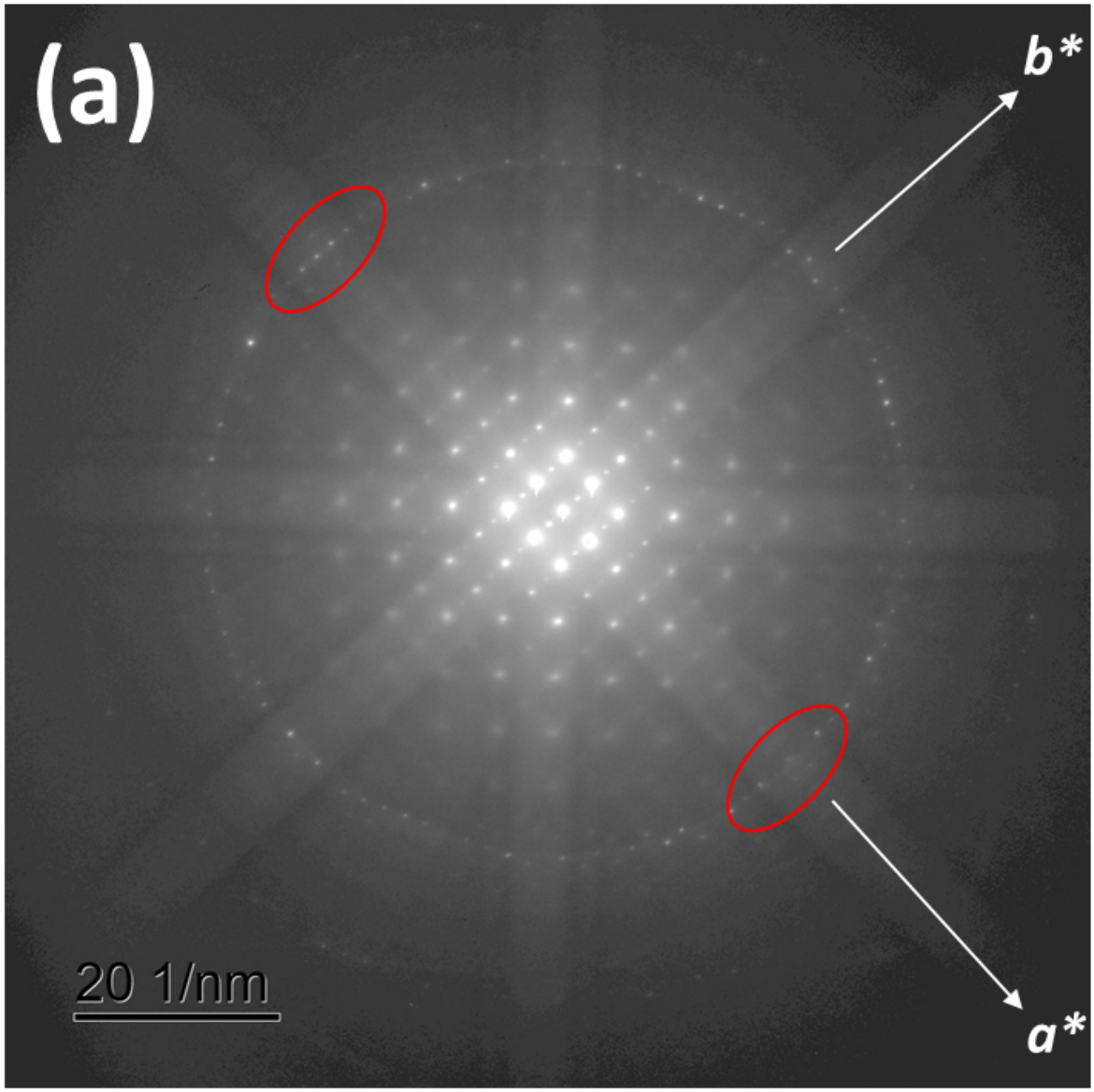

Fig. S5a

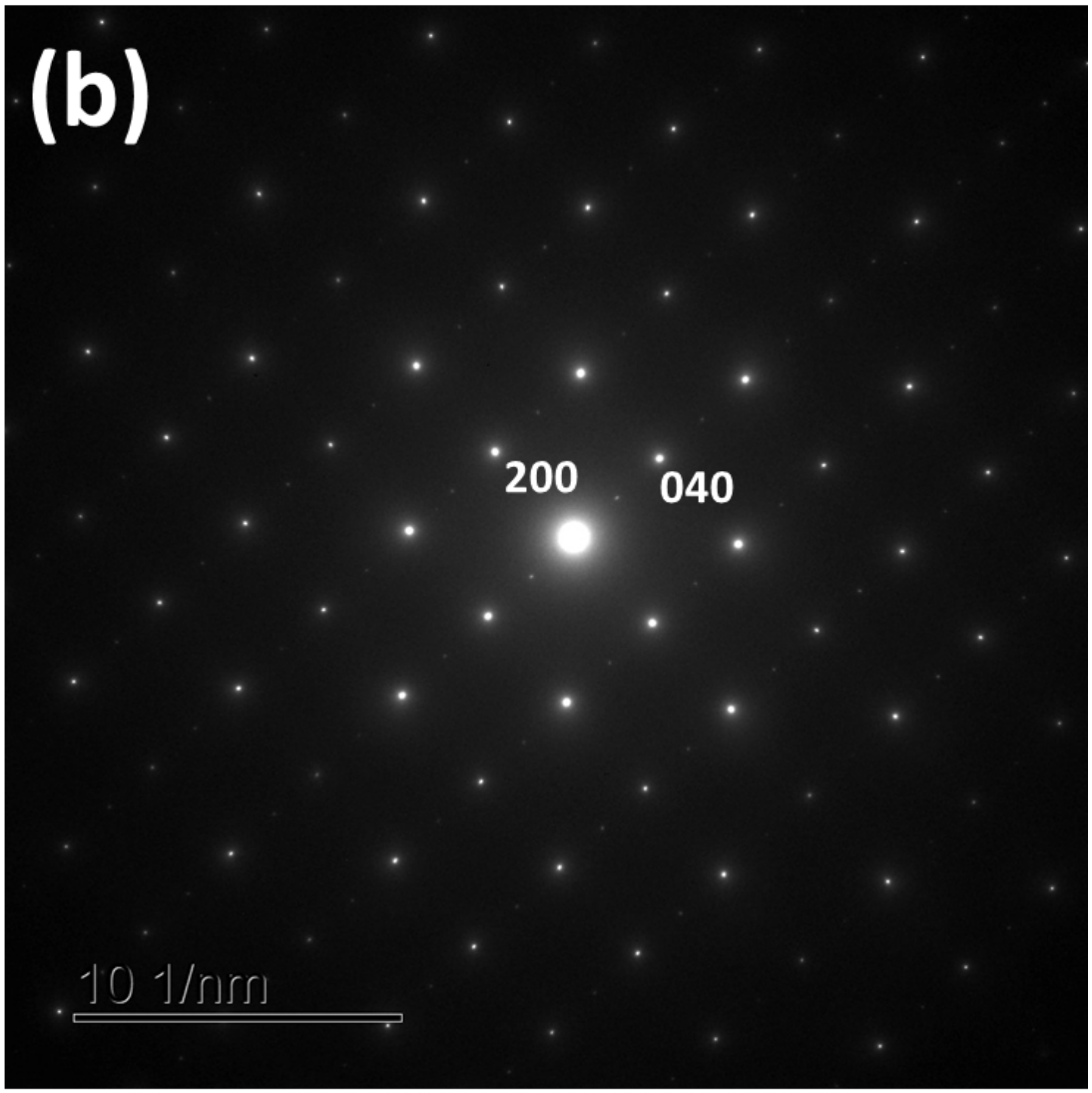

Fig. S5b

Supplemental Fig. S5. (a) HOLZ pattern of the [001] zone axis of wadsleyite with a camera length (CL) of 86 mm in a FEI Titan G2 80-200 TEM for reproducibility. As in Fig. 7a, intensity distributions along the *a* axis (red ellipses) are incompatible with a mirror plane perpendicular to the *a* axis despite of using different measuring conditions and different TEM instruments. (b) The corresponding PsSAED pattern with CL of 255 mm. The precession angle is 3°. It displays no detectable intensities of *hk*0 reflections with $h, k = 2n + 1$ in this pseudo-kinematical diffraction condition.

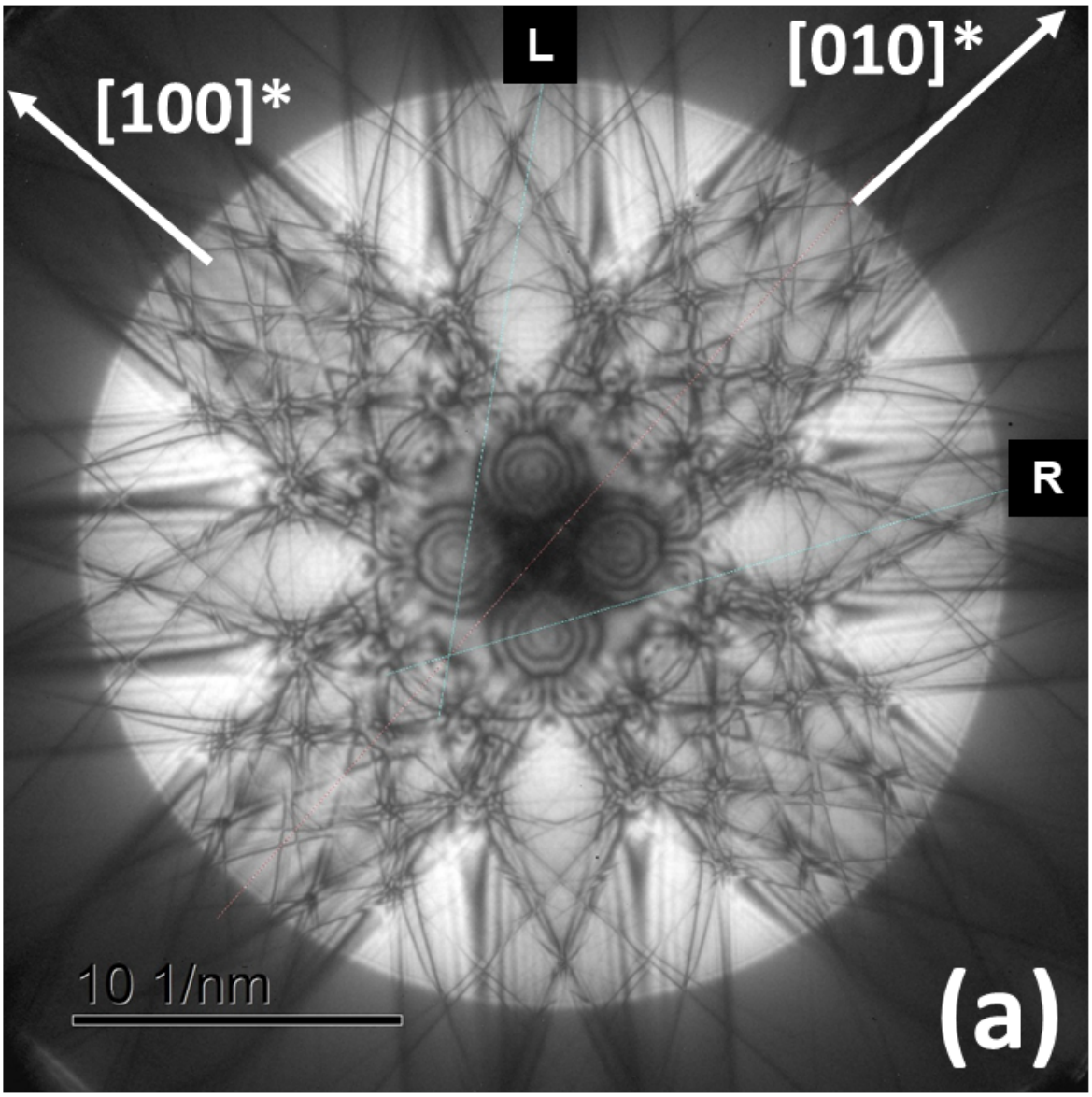

Fig. S6a

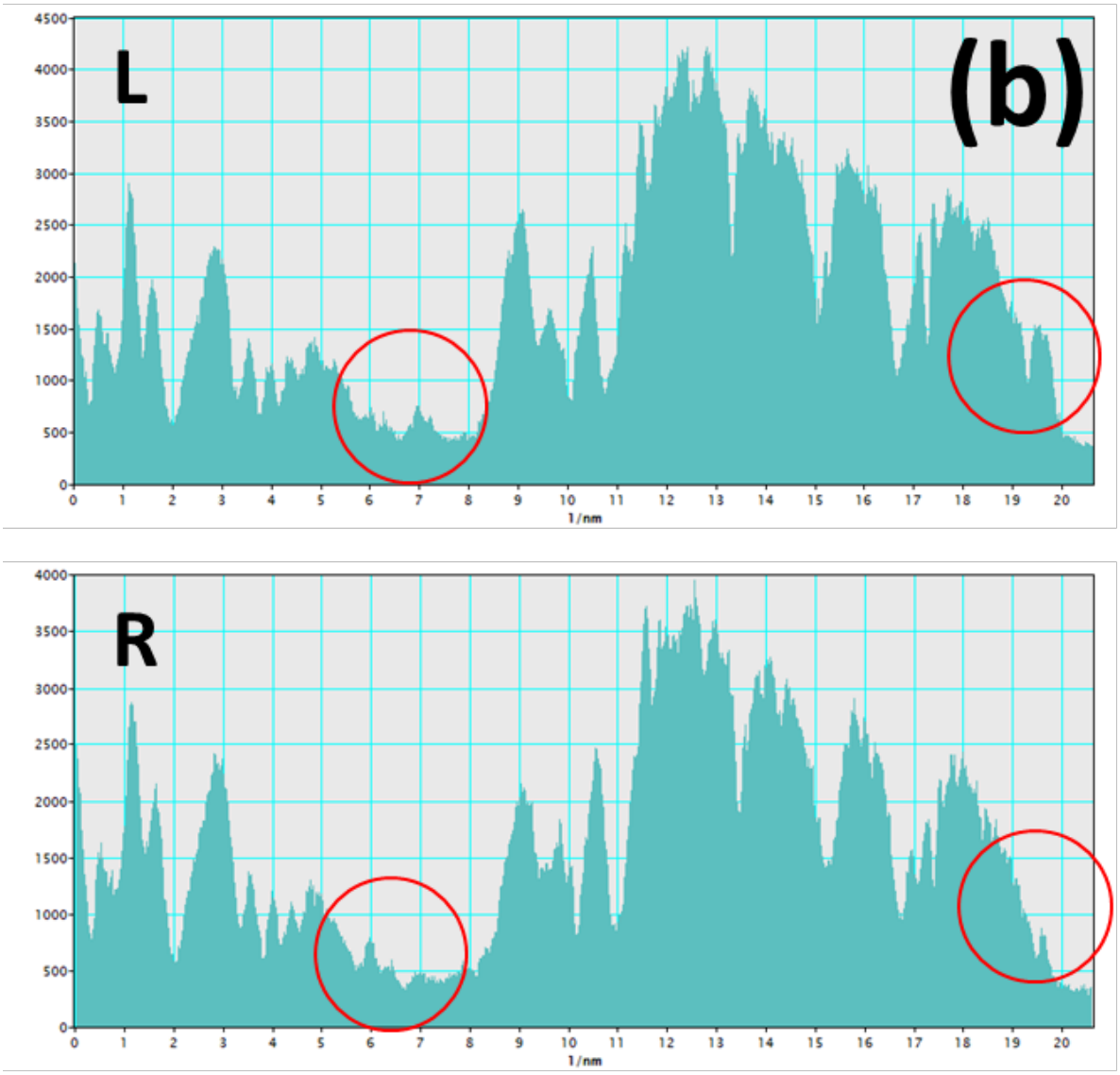

Fig. S6b

Supplemental Fig. S6. (a) LACBED pattern taken along the [001] zone axis of wadsleyite. The crystal orientation for the diffraction is the same as that of Fig. S4. The convergent angle is more than 100 mrad (~ 5 °). (b) The intensity profiles along the lines “R” and “L” in the LACBED pattern (a) are plotted to check for mirror symmetry along the [100] direction. The profiles are almost identical except for the red circled areas.

References for the Supplemental information

Seto, Y., and Ohtsuka, M. (2022) ReciPro: free and open-source multipurpose crystallographic software integrating a crystal model database and viewer, diffraction and microscopy simulators, and diffraction data analysis tools. Journal of Applied Crystallography, 55, 1-15.